Semiconductor Physics, Quantum Electronics & Optoelectronics, 2021. V. 24, No 4. P. 399-406.

Semiconductor physics

Reduction of reverse leakage current at the TiO_2/GaN interface in field plate Ni/Au/*n*-GaN Schottky diodes

B.N. Shashikala[1], B.S. Nagabhushana[2]

[1]*Siddaganga Institute of Technology, Tumakuru, India*
[2]*BMS College of Engineering, Bengaluru, India*
E-mail: shashikala.bn@gmail.com

Abstract. This paper presents the fabrication procedure of TiO_2 passivated field plate Schottky diode and gives a comparison of Ni/Au/*n*-GaN Schottky barrier diodes without field plate and with field plate of varying diameters from 50 to 300 µm. The influence of field oxide (TiO_2) on the leakage current of Ni/Au/*n*-GaN Schottky diode was investigated. This suggests that the TiO_2 passivated structure reduces the reverse leakage current of Ni/Au/*n*-GaN Schottky diode. Also, the reverse leakage current of Ni/Au/*n*-GaN Schottky diodes decreases as the field plate length increases. The temperature-dependent electrical characteristics of TiO_2 passivated field plate Ni/Au/*n*-GaN Schottky diodes have shown an increase of barrier height within the temperature range 300…475 K.

Keywords: field plate, GaN, leakage current, Schottky diode, TiO_2.

https://doi.org/10.15407/spqeo24.04.399
PACS 85.30.Hi, 85.30.Kk

Manuscript received 27.09.20; revised version received 27.07.21; accepted for publication 10.11.21; published online 23.11.21.

1. Introduction

GaN as a base material for high power, high temperature, and high-frequency devices has demonstrated its great potential over the past recent years. The physical background of this potential is given by its superior material properties such as wide bandgap, high breakdown electric field, and high-saturation electron drift velocity [1–4]. Important for power devices, the 10-fold increase in the critical field of GaN allows high-voltage blocking layers to be approximately 10-fold thinner than those of Si-based devices, thus reducing the device on-resistance and power losses when maintaining the same high blocking capability. Unfortunately, breakdown voltages for planar junctions suffer from an acute reduction due to well-known device edge field crowding effect [5], limiting the potential performance of GaN power devices. Development of proper edge termination to relieve this effect and reaching a breakdown voltage close to the ideal one is one of the most important aspects of device design and processing. It represents a current research field. Several edge termination structures for GaN devices have been investigated, involving field plates (FPs), guard rings, finite termination by argon implantation, implanting a neutral species on the edges of devices, and junction termination extensions (JTE) [6–16]. Among all of these edge termination structures, field plate termination offers an attractive advantage of simple processing steps when compared with other edge termination techniques.

An interesting attribute of field plate dielectric is the dielectric constant which tune the potential spread in a field plate terminated structures similar to overlap length. High-K dielectric TiO_2 generates a greater expanded depletion region than that generated using SiO_2 or SiN_x film of the same thickness. The overlap required for maximizing the potential spread reduces with the increase in dielectric constant.

For practical applications, the precise control of the crystal phase of TiO_2 by sputtering at different temperatures is important for passivation of devices [17]. The preferred orientation and phase composition could be controlled by adjusting the bias voltage at different temperatures.

In this paper, the details of experimental work of Ni/Au/*n*-GaN Schottky diode and TiO_2 passivated field plate structures are present in Section 2. The characterization study includes measurement of current-voltage (*I*–*V*) characteristics of Ni/Au/*n*-type GaN Schottky barrier diode and TiO_2 passivated field plate Ni/Au/*n*-GaN Schottky diode are discussed in Section 3. Also, the influence of the field plate length on the leakage current is discussed.

© 2021, V. Lashkaryov Institute of Semiconductor Physics, National Academy of Sciences of Ukraine

2. Fabrication procedure

2.1. GaN Schottky diode

A doped *n*-type (N_D^+ approximately $1\cdot10^{18}$ cm^{-3} by Hall measurement) GaN layer of 5 µm grown by MOCVD on *c*-plane sapphire substrate was used for the experiment. Prior to metal deposition, a sample was cleaned in trichloroethylene (TCE) to degrease and then treated using acetone for further cleaning. The sample was then immersed in isopropyl alcohol (IPA) for complete removal of organic solvents. It was then well rinsed in deionized water (DI) and ready for removal of ionic contaminants and native oxide. It was then immersed in an equally proportioned solution of dilute HCl in DI water. After this treatment for 5 min, the sample was rinsed again in DI water and blow dried using N_2 gas. Fig. 1 shows the structure of the sample and the metal contact. All the metal contacts were fabricated with the standard photolithographic lift-off technique with a positive photoresist. For the Ohmic contact, Ti/Al/Ni/Au (20 nm/60 nm/20 nm/50 nm, with the Ti layer at the bottom) films were deposited on the wafer by electron-beam (e-beam) evaporator and annealed using rapid thermal annealing (RTA) technique at the temperature close to 850 °C for 30 s. Ni/Au (50 nm/50 nm) was deposited on the wafer by e-beam evaporator, to form the Schottky contact. The Ohmic contacts were circles having an inner radius of r_2 (180 µm) and external radius of r_3 (255 µm), and the Schottky contact was dot with the radius r_1 (150 µm) at the center. Schottky contacts of different sizes (diameter ranging from 50 to 300 µm) were deposited on the samples. The electrical characteristics of the fabricated Schottky diodes were investigated using *I–V* measurements with Keithley 4200.

2.2. Field plate GaN Schottky diode

The doped *n*-type GaN layer of the 5-µm thickness grown by MOCVD on *c*-plane of sapphire substrate was used for the experiment. Prior to metal deposition, a sample was cleaned in TCE, acetone, IPA, HCl and then rinsed in DI water and blow dried using N_2 gas. The 15-nm thick TiO_2 dielectric was deposited by sputter. Windows were opened in the TiO_2 dielectric by etching using $HF:H_2O_2$ (5:1). All the metal contacts were fabricated with the standard photolithographic and lift-off technique with a positive photoresist. For the Ohmic contact, Ti/Al/Ni/Au (20 nm/60 nm/20 nm/50 nm, with the Ti layer at the bottom) films were deposited on the wafer by e-beam evaporator and annealed using RTA technique at the temperature 850 °C for 30 s. Ni/Au (50 nm/50 nm) was deposited on the wafer by e-beam evaporator, to form the Schottky contact. Fig. 2 shows the schematic of the Ni/Au/*n*-GaN Schottky diode with field plate. The electrical characteristics of the fabricated field plate Schottky diode were investigated also using *I–V* measurements with Keithley 4200.

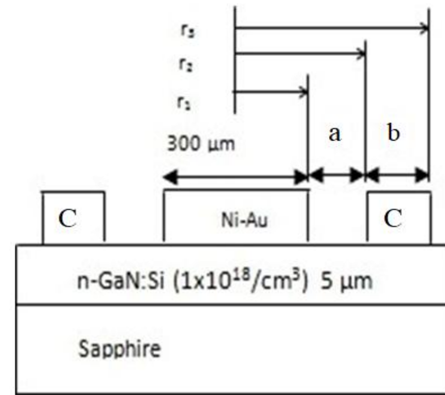

Fig. 1. Schematic cross-section of the 300-µm Ni/Au/*n*-GaN Schottky barrier diode without the field plate. C – Ti/Al/Ni/Au (20 nm/60 nm/20 nm/50 nm), a = 30 µm, b = 75 µm.

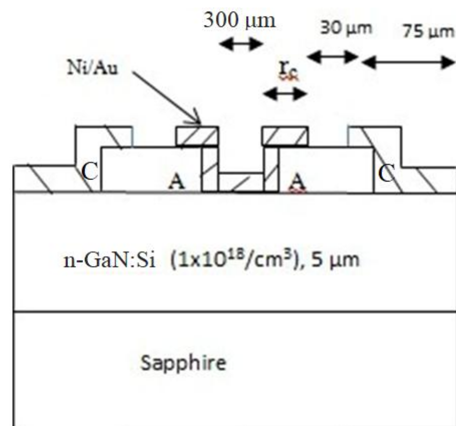

Fig. 2. Schematic cross-section of the Ni/Au/*n*-GaN Schottky diode with the field plate. A – TiO_2, C – Ti/Al/Ni/Au (20 nm/60 nm/20 nm/50 nm), r_c = 5, 10, 15, 20 µm.

3. Results and discussion

3.1. Analysis of current–voltage–temperature (*I–V–T*) characteristics in the forward bias

Fig. 3 shows the forward and reverse bias current-voltage characteristics of the 300 µm Ni/Au/*n*-GaN Schottky barrier diodes without field plate and TiO_2 field plate. Direct current *I–V* measurements indicate that the forward current is lower for TiO_2 (15 nm) passivated Schottky diode with metal overlap edge termination than those of unterminated Schottky diode. The forward current at 1 V for the unterminated diode is close to $30\cdot10^{-6}$ A while that for TiO_2 passivated Schottky diode is $2.83\cdot10^{-6}$ A. This decrease in the current is attributed to the reduction in surface leakage between the Schottky and Ohmic contacts. When the main Schottky contact is in reverse bias, the depletion region of the main Schottky junction is increased. The leakage current of SBDs without any edge termination is high due to the electric field crowding under the edge of the Schottky junction.

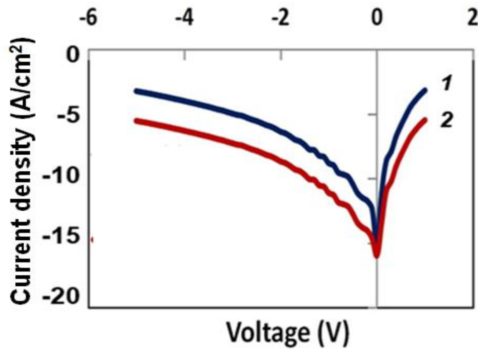

Fig. 3. Forward and reverse *I–V* characteristics of the 300-µm Ni/Au/*n*-GaN Schottky barrier diodes without the field plate (*1*) and with the TiO_2 passivated field plate (*2*).

The electric field under the main Schottky junction is distributed and reduced due to the field plate. The leakage current of the field-plate terminated SBDs is decreased due to the reduction of electric field crowding of Schottky junction. It is noted that the leakage current without field plate ($13.2\cdot10^{-6}$ A) decreases with the TiO_2 passivated Schottky diode ($1.34\cdot10^{-6}$ A) at –4 V as shown in Fig. 3.

3.2. Analysis of *I–V–T* characteristics in the forward bias

Fig. 4 shows the forward and the reverse bias current-voltage characteristics of 300-µm Ni/Au/*n*-GaN Schottky barrier diode with field plate within the temperature range 300…475 K. The current-voltage-temperature characteristics are widely used to study the performance of the Schottky contacts since many important device parameters may be extracted. The *I–V* characteristics based on the thermionic emission (TE) theory are given by the relation [18]

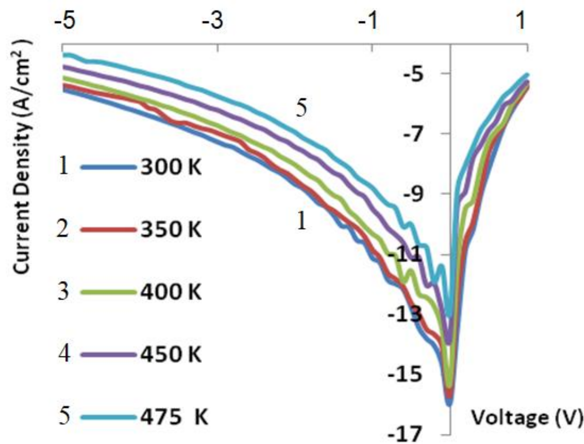

Fig. 4. Forward and reverse *I–V* characteristics of the 300-µm Ni/Au/*n*-GaN Schottky barrier diodes with the field plate as a function of temperature.

$$I = I_0\left[\exp\left(\frac{qV}{nkT}\right)-1\right], \tag{1}$$

where V is the applied voltage drop across the junction barrier in Volts, q – electronic charge, k – Boltzmann constant, T – absolute temperature in Kelvin, n – diode ideality factor, and I_0 – saturation current that is expressed as

$$I_0 = AA^*T^2\exp\left(\frac{-q\varphi_{bo}}{kT}\right), \tag{2}$$

where A is the diode area, φ_{bo} – barrier height, and A^* – effective Richardson constant (26.4 $A\cdot cm^{-2}K^{-2}$) based on effective mass ($m^* = 0.22m_0$) of *n*-GaN [19]. The values of the barrier height and ideality factor (n) for the device are determined from the y intercepts and slopes of the forward bias ln(J) *vs* V plot at each temperature, respectively. The barrier height can be obtained by rewriting (2) as

$$\varphi_{bo} = \frac{kT}{q}\ln\left(\frac{AA^*T^2}{I_0}\right). \tag{3}$$

The ideality factor n is a measure of conformity of the diode to pure thermionic emission and the thermionic emission is inferred to be of the purest order, if n is equal to one. However, n has usually a value greater than unity. The value of ideality factor n is given by

$$n = \frac{q}{kT}\left(\frac{dV}{d(\ln I)}\right). \tag{4}$$

It is observed that the leakage current increases with the increase in temperature within the range $2.95\cdot10^{-6}$ A (at 300 K) to $2.36\cdot10^{-5}$ A (at 475 K) at –1V. It is noted that the extracted barrier height increased from 0.79 to 1.21 eV with the increase in temperature from 300 to 475 K, accompanied by a significant improvement of the ideality factor n from 2.18 to 1.6. As shown in Fig. 5, both increase in φ_{bo} and decrease in n are expected with increase in temperature as contribution from TE component to the total current increases. The interface quality depends on several factors, namely: surface treatment (cleaning, etching, *etc.*), deposition processes (evaporation, sputtering, *etc.*), surface defect density, and local enhancement of electric field, which can also yield a local reduction of SBH. This leads to inhomogeneity in the transport current. The existence of Schottky barrier height inhomogeneity was used to explain this temperature dependence of φ_{bo} and n [20]. A diode is assumed to consist of parallel segments of different barrier heights and each contributes to the current independently, the current of the diode will preferentially flow through the lower barriers. As a result, the current conduction is dominated by patches of lower barrier height with a larger ideality factor at lower temperatures. However, as the temperature increases, patches with higher barrier heights influence due to the fact that electrons gain sufficient thermal energy to surmount them [21]. The ideality factor greater than unity indicate that Schottky diode exhibits non-ideal current behavior.

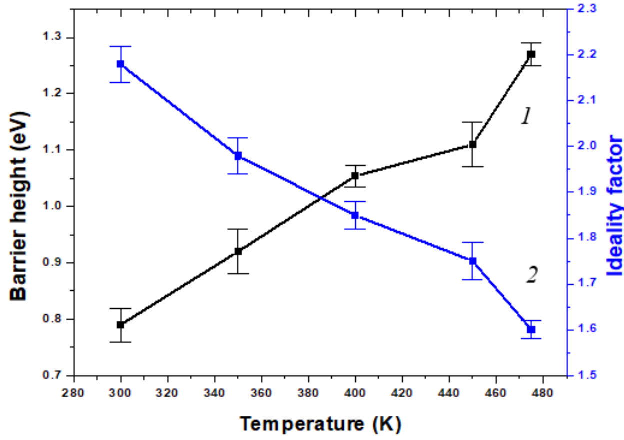

Fig. 5. Temperature dependence of the barrier height (*1*) and ideality factor (*2*) for Ni/Au/*n*-GaN SBD extracted from *I–V* characteristics.

The Richardson constant is usually determined from the $\ln(I_0/T^2)$ *vs* $1/T$ plot, where I_0 is the saturation current. Eq. (2) can be written as

$$\ln\left(\frac{I_0}{T^2}\right) = \ln\left(AA^*\right) - \frac{q\varphi_{bo}}{kT} . \tag{5}$$

The plot of $\ln(I_0/T^2)$ *vs* $q/(kT)$ should be linear for TE, as well as A^* and φ_{bo} are the intercept and slope, respectively. This is not true for inhomogeneous diodes. A modified activation energy expression according to the Gaussian distribution of SBHs can be written as [22]

$$\ln\left(\frac{I_0}{T^2}\right) - \frac{q^2\sigma_s^2}{2k^2T^2} = \ln\left(AA^*\right) - \frac{q\varphi_{bo}}{kT} , \tag{6}$$

where extracted standard deviation σ_s is 0.2 V. The slope of the plot of φ_{bo} *vs* $q/2kT$ gives the square of standard deviation. The value of A^* obtained from the intercept of this straight line portion at the ordinate of the experimental $\left[\ln\left(I_0/T^2\right) - 1/2\left(q\sigma_s/kT\right)^2\right]$ *vs* $q/(kT)$ plot in Fig. 6 is equal to 32 $\text{A·cm}^{-2}\text{K}^{-2}$, which is closer to 26 $\text{A·cm}^{-2}\text{K}^{-2}$. The deviation in the Richardson constant may be due to the influences of the image force, tunneling current through the potential barrier, recombination in the space charge region appearing at low voltage and variation of the charge distribution near the interface [23]. According to Horvath [24], the value of A^* obtained from the temperature dependence of the *I–V* characteristics may be affected by the lateral inhomogeneity of the barrier, too.

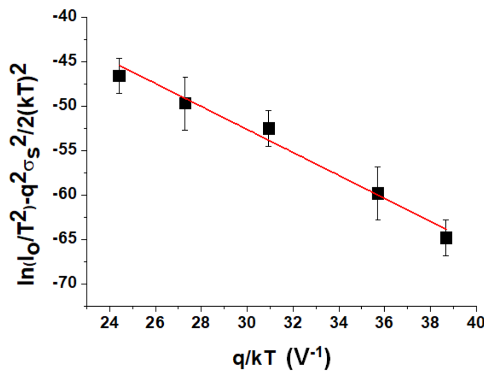

Fig. 6. Modified Richardson plot of $\left[\ln\left(I_0/T^2\right) - q^2\sigma_s^2/2k^2T^2\right]$ *vs* q/kT for Ni/Au/*n*-GaN SBD.

3.3. Analysis of *I–V–T* characteristics in the reverse bias

The reverse current (I_0) is much higher than that predicted by TE. Hence, other mechanisms may be present. As reported in the literature, Frenkel–Poole emission (FPE) is considered. The high leakage currents in reverse-biased Schottky contacts to *n*-type GaN are related to threading screw dislocations [25]. The main mechanism for high leakage current occurs through FPE. This leakage current is governed by the emission of electrons *via* trap state into a continuum of states associated with the presence of conductive dislocations. In FPE model, emission of electron refers to the electrical-field-enhanced thermal emission from a trap state into a continuum of electronic states. The current density associated with FPE [26] is given by

$$J = KE_r \exp\left[-\frac{q\left(\varphi_t - \sqrt{\frac{qE_r}{\pi\varepsilon_s\varepsilon_0}}\right)}{kT}\right] , \tag{7a}$$

$$E_r = \sqrt{\left(\varphi_i - V - kT\right)\frac{2qN_D}{\varepsilon_0\varepsilon_s}} \quad [23], \tag{7b}$$

$$\varphi_i = \varphi_m - \varphi_s , \tag{7c}$$

where K is a constant, E_r – electric field in the semiconductor barrier at the metal/semiconductor interface, φ_t – barrier height for electron emission from the trap state, ε_s – relative permittivity at high frequency, ε_0 – permittivity of free space, φ_i – built-in voltage, φ_m – metal work function voltage, φ_s – semiconductor work function voltage. From Eq. (7a), $\ln(J/E_r)$ should be a linear function of $\sqrt{E_r}$, *i.e.*,

$$\ln\left(\frac{J}{E_r}\right) = \frac{q}{kT}\sqrt{\frac{qE_r}{\pi\varepsilon_s\varepsilon_0}} - \frac{q\varphi_t}{kT} + \ln K = m(T)\sqrt{E_r} + b(T) , \tag{8a}$$

where

$$m(T) = \frac{q}{kT}\sqrt{\frac{q}{\pi\varepsilon_s\varepsilon_0}} \ , \qquad (8b)$$

$$b(T) = -\frac{q\varphi_t}{kT} + \ln K \ . \qquad (8c)$$

The measured macroscopic current densities in GaN Schottky diode are observed to be dependent on both electric field and temperature. Fig. 7 shows the plot of $\ln(J/E_r)$ *vs* E_r as linear within the temperature range 300…475 K for Pd Schottky contact on GaN. This indicates the presence of Frenkel–Poole emission in Pd Schottky contacts on GaN. Further, Fig. 8 shows the plot of $b(T)$ as defined in Eq. (8c), plotted as a function of (q/kT). The calculated emission barrier height φ_t from the slope of $b(T)$ *vs* (q/kT) is 0.16 ± 0.02 eV. The extracted value of φ_t for GaN is in good agreement with the previously reported values [26].

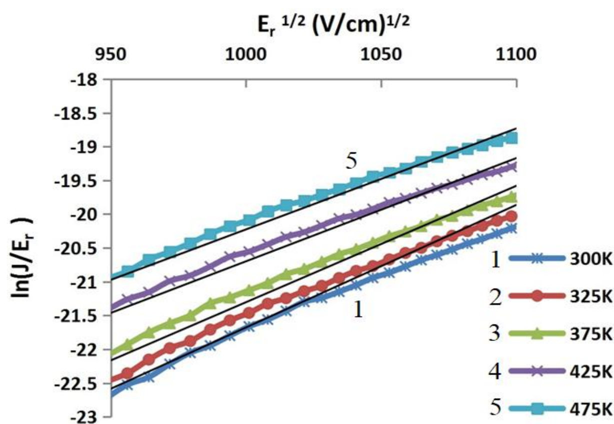

Fig. 7. The plot of $\ln(J/E_r)$ *vs* $\sqrt{E_r}$.

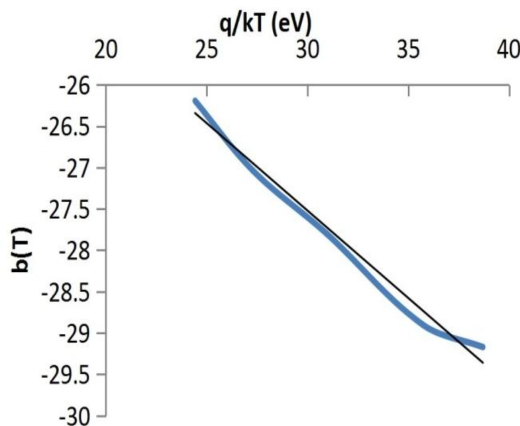

Fig. 8. Slopes of $b(T)$ vs q/kT.

3.4. Current density dependence on diode area

The circular Schottky diodes with diameters varying from 50 to 300 µm were tested to investigate the effect of diode area and perimeter on the current density. The influence of perimeter/area ratio on diode current density is as shown in Fig. 9. As seen in Fig. 9a, increasing the perimeter/area ratio increases the current density in the forward bias at 1 V. In Fig. 9b, the plot of reverse current density as a function of the perimeter/area ratio shows an increasing trend at –1 V. From Fig. 9b, it is clear that the reverse leakage current is dependent on the perimeter of the device. This perimeter dependence suggests the considerable contribution of the surface leakage. Since the dimensions of the device reduce, the surface effects should dominate over the bulk ones. So for smaller devices the major component of the current is the current flowing along the surface. This surface current depends on the perimeter rather than the area of the device. This may be due to surface recombination or surface channel formation.

An estimation of the contribution of surface leakage to the total leakage current of Schottky diodes is made. The reverse leakage current of the Schottky diode can be expressed as [27]

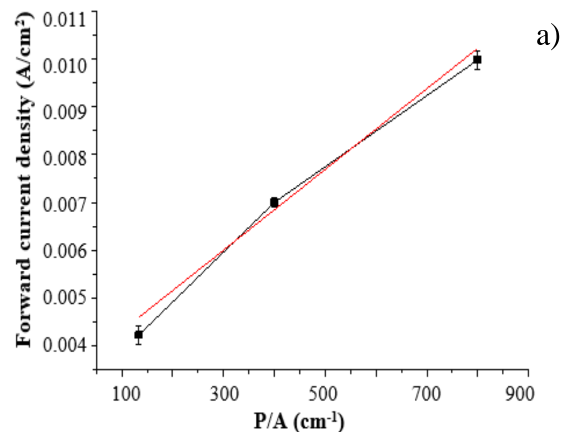

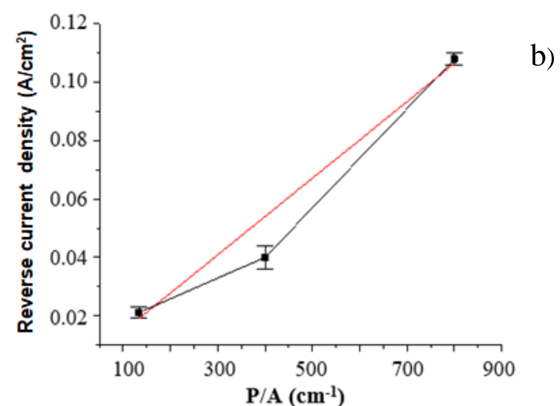

Fig. 9. Dependences of current density on the diode perimeter/area ratio at the forward (a) and reverse (b) bias.

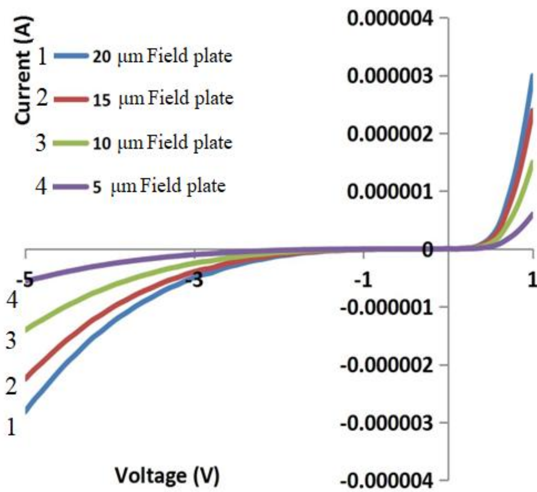

Fig. 10. Forward and reverse *I–V* characteristics of the TiO_2 passivated field plate Ni/Au/*n*-GaN Schottky barrier diode as a function of field plate length, μm: *1* – 5, *2* – 10, *3* – 15, *4* – 20.

$$\frac{I_0}{A} = J_B + J_s \frac{P}{A}, \tag{9}$$

where J_B is the density of current flowing into the bulk of GaN at Schottky interface, J_s – surface leakage current density, *P* and *A* are the perimeter and area of the device respectively, J_B – leakage current component per unit area of the device with the dimension of $A\ \mathrm{cm}^{-2}$. J_s is defined as the surface leakage current per unit perimeter of the device with the dimension of $A\ \mathrm{cm}^{-1}$. The current due to J_B is proportional to the area of the device. On the other hand, the surface leakage current is proportional to the perimeter of the device. The plot of reverse current density I_0/A *versus* P/A from Eq. (9) will be a straight line, which slope is the surface leakage current density. The value of J_B extracted from the current density *vs* P/A is 5.47 ± 0.04 mA/cm^2 and J_s is equal to 0.15 ± 0.09 mA/cm.

Fig. 10 shows the forward and reverse bias current-voltage characteristics of 300-μm Ni/Au/*n*-GaN Schottky barrier diodes with TiO_2 field plate of different sizes (5, 10, 15, and 20 μm). The measurement results showed that the forward current increases and the reverse leakage current decreases as the field plate length increases.

4. Conclusions

Leakage current reduction in Ni/Au/*n*-GaN Schottky diode was achieved by utilizing TiO_2 passivated field-plate termination. The forward current was decreased in the TiO_2 passivated field-plate terminated diode due to formation of an accumulation layer in GaN, underneath the metal and in the region where the metal overlaps the oxide. It was noted that the leakage current of unterminated diode decreases with the TiO_2 passivated field-plate terminated diode. The forward current of the TiO_2 passivated field-plate terminated diode increases, and the reverse leakage current decreases with increasing the field plate length. The analysis of the current-voltage characteristics of the TiO_2 passivated field-plate terminated Ni/Au/*n*-GaN Schottky diode have shown an increase of barrier height accompanied by improvement of the ideality factor. The emission barrier height is 0.16 ± 0.02 eV. The current-voltage characteristics of the TiO_2 passivated field-plate terminated Ni/Au/*n*-GaN Schottky diodes from 50 to 300 μm have shown the major reverse current flows along the surface for smaller devices.

Acknowledgements

The authors would like to thank the staff members of the Indian Nanoelectronics Users Program for their support during the fabrication process. The experiments in this paper were carried out at Indian Institute of Technology, Bombay, under the Indian Nanoelectronics Users Program.

References

1. Tian J., Lai C., Feng G. *et al.* Review of recent progresses on Gallium Nitride transistor in power conversion application. *Int. J. Sustainable Energy*. 2020. **39**, No 1. P. 88–100. https://doi.org/10.1080/14786451.2019.1657866.
2. Zhang A., Zhou Q., Yang C. *et al.* A high-accuracy AlGaN/GaN reverse blocking CRT with hybrid trench cathode. *Nanoscale Res. Lett*. 2019. **14**. Article No. 23. https://doi.org/10.1186/s11671-019-2860-y.
3. Azurza A.J., Zulauf G.D., Kolar J.W. and Deboy G. New figure-of-merit combining semiconductor and multi-level converter properties. *IEEE Open Journal of Power Electronics*. 2020. **1**. P. 328–338. https://doi.org/10.1109/OJPEL.2020.3018220.
4. Jiya N. and Gouws R. Overview of power electronic switches: A summary of the past, state-of-the-art and illumination of the future. *Micromachines*. 2020. **11**. P. 2–29. https://doi.org/10.3390/mi11121116.
5. Baliga B.J. *Fundamentals of Power Semiconductor Devices*. New York, 2019.
6. Bahat-Treidel E., Hilt O., Zhytnytska R. *et al*. Fast-switching GaN-based lateral power Schottky barrier diodes with low onset voltage and strong reverse blocking. *IEEE Electron Device Lett*. 2012. **33**, No 3. P. 357–359. https://doi.org/10.1109/LED.2011.2179281.
7. Merve Ozbek A., Baliga B.J. Finite-zone argon implant edge termination for high-voltage GaN Schottky rectifiers. *IEEE Electron Device Lett*. 2011. **32**, No 10. P. 1367–1369. https://doi.org/10.1109/LED.2011.2162221.
8. Sundaramoorthy V.K., Nistor I. Study of edge termination structures for high power GaN Schottky diodes. *phys. status solidi C*. 2011. **8**, No 7/8. P. 2270–2272. https://doi.org/10.1002/pssc.201001032.
9. Sun Y., Kang X., Zheng Y. *et al*. Review of the recent progress on GaN-based vertical power Schottky barrier diodes. *Electronics*. 2019. **8**, No 5. P. 575. https://doi.org/10.3390/electronics8050575.

10. Han S., Song J., and Chu R. Design of GaN/ AlGaN/GaN super-heterojunction Schottky diode. *IEEE Trans. Electron Devices*. 2020. **67**, No 1. P. 69–74. https://doi.org/10.1109/TED.2019.2953843.
11. Zhang Y., Lu X., and Zou X. Device design assessment of GaN merged *p-i-n* Schottky diodes. *Electronics*. 2019. **8**. P. 1550–1561. https://doi.org/10.3390/electronics8121550.
12. Suemitsu T., Kobayashi K., Hatakeyama S. A new process approach for slant field plates in GaN, based high-electron-mobility transistors. *Jpn. J. Appl. Phys*. 2016. **55**, No 2. P. 01AD02–06. https://doi.org/10.7567/JJAP.55.01AD02.
13. Yang J., Ahn S., Ren F. *et al*. High reverse breakdown voltage Schottky rectifiers without edge termination on Ga_2O_3. *Appl. Phys. Lett*. 2017. **110**. P. 192101–4. https://doi.org/10.1063/1.4983203.
14. Ma J., Matioli E. Field plate design for low leakage current in lateral GaN power Schottky diodes: Role of the pinch-off voltage. *IEEE Electron Device Lett*. 2017. **38**, No 9. P. 1298–1301. https://doi.org/10.1109/LED.2017.2734644.
15. Wong J., Shinohara K., Corrion A.L *et al*. Novel asymmetric slant field plate technology for high-speed low-dynamic R_{on} E/D-mode GaN HEMTs. *IEEE Electron Device Lett*. 2017. **38**, No. 1. P. 95–98. https://doi.org/10.1109/LED.2016.2634528.
16. Cucak D., Vasic M., Garcia O. *et al*. Physics-based analytical model for input, output and reverse capacitance of a GaN HEMT with the field-plate structure. *IEEE Trans. Power Electron*. 2017. **32**, No 3. P. 2189–2202.
17. Zhu X., Gu P., Wu H. *et al.* Influence of substrate on structural, morphological and optical properties of TiO_2 thin films deposited by reaction magnetron sputtering. *AIP Adv*. 2017. **7**. P. 1253261–8. https://doi.org/10.1063/1.5017242.
18. Lee M., Ahn C.W., Vu T.K.O. *et al*. Current transport mechanism in palladium Schottky contact on Si-based freestanding GaN. *Nanomaterials.* 2020. **10**. P. 297–303. https://doi.org/10.3390/nano10020297.
19. Sadao Adachi. *Properties of Semiconductor Alloys: Group-IV, III-V and II-VI Semiconductors*. Japan, Wiley, 2009.
20. Garg M., Kumar A., Sun H., Liao C., Li X., and Singh R. Temperature dependent electrical studies on Cu/AlGaN/GaN Schottky barrier diodes with its microstructural characterization. *Journal of Alloys and Compounds*. 2019. **806**. P. 852–857. https://doi.org/10.1016/j.jallcom.2019.07.234.
21. Akkaya A. and Ayyildiz E. Effects of post annealing on *I-V-T* characteristics of (Ni/Au)/$Al_{0.09}Ga_{0.91}N$ Schottky barrier diodes. *J. Phys. Conf. Series*. 2016. **707**. P. 012015. https://doi.org/10.1088/1742-6596/707/1/012015.
22. Reddy D.S., Reddy M.B., Nanda N. *et al*. Schottky barrier parameters of Pd/Ti contacts on *n*-type InP revealed from *I-V-T* and *C-V-T* measurements. *J. Modern Phys*. 2011. **2**. P. 113–123. https://doi.org/10.4236/jmp.2011.23018.
23. Thao C.P., Kuo D.H. Electrical and structural characteristics of Ge-doped GaN thin films and its hetero-junction diode made all by RF reactive sputtering. *Mater. Sci. in Semiconductor Proc.* 2018. **74**. P. 336–341. https://doi.org/10.1016/j.mssp.2017.10.024.
24. Rao P.K., Park B.-G., Lee S.-T., Kim M.-D., Oh J.-E. Temperature-dependent electrical properties of (Pt/Au)/Ga-polarity GaN/Si(111) Schottky diode. *Microelectron. Eng*. 2012. **93**. P. 100–104. https://doi.org/10.1016/j.mee.2011.11.019.
25. Alshahed M., Heuken L., Alomari M. *et al.* Low-dispersion, high-voltage, low-leakage GaN HEMTS on native GaN substrates. *IEEE Trans. Electron Devices*. 2017. **14**, No. 8. P. 1–8.
26. Rao P.K., Park B., Lee S.-T., Noh Y.-K., Kim M.-D., and Oh J.-E. Analysis of leakage current mechanisms in Pt/Au Schottky contact on Ga-polarity GaN by Frenkel-Poole emission and deep level studies. *J. Appl. Phys.* 2011. **110**. P. 013716. https://doi.org/10.1063/1.3607245.
27. Kim H., Lee D.H., and Myung H.S. Contact area-dependent electron transport in Au/*n*-type Ge Schottky junction. *Korean Journal of Materials Research*. 2016. **26**, No. 8. P. 412–416. https://doi.org/10.3740/MRSK.2016.26.8.412.

Authors and CV

B.N. Shashikala, Associate Professor of Department of Electronics and Communication, Siddaganga Institute of Technology, Tumkur. She received ME degree from Gulbarga University and PhD degree. Since 1994, she has been in Electronics and Communication Engineering Department, SIT, Tumkur. Her research interests are in III-V electronics and devices technology, and power electronics devices.

B.S. Nagabhushana, Professor of Post Graduate Studies in Electronics at BMS College of Engineering, Bengaluru. He received PhD in Electrical Sciences, Indian Institute of Science, Bangalore in 1999. He has professional experience of 25 years, with a mix of teaching, industrial and research. His present researches include automotive electronics and semiconductor technologies.

Зменшення зворотного струму витоку на межі TiO_2/GaN у Ni/Au/*n*-GaN діодах Шоттки з пасивуючим шаром TiO_2

B.N. Shashikala, B.S. Nagabhushana

Анотація. Наведено процедуру виготовлення діода Шотткі з охоронним кільцем з пасивуючим шаром TiO_2, а також порівняно бар'єрні діоди Шотткі Ni/Au/*n*-GaN без охоронного кільця та з ним різних діаметрів від 50 до 300 мкм. Досліджено вплив пасивуючого оксиду (TiO_2) на струм витоку у діоді Шотткі Ni/Au/*n*-GaN. Це свідчить про те, що пасивуюча TiO_2 структура зменшує зворотний струм витоку у діоді Шотткі Ni/Au/*n*-GaN. Також зворотний струм витоку у діодах Шотткі Ni/Au/*n*-GaN зменшується із збільшенням розмірів охоронного кільця. Температурно-залежні електричні характеристики діодів Шотткі Ni/Au/*n*-GaN з охоронним кільцем з пасивуючим шаром TiO_2 показали збільшення висоти бар'єра в діапазоні температур 300…475 K.

Ключові слова: пасивуючий шар TiO_2, GaN, струм витоку, діод Шотткі.